Available online at website: https://journal.bcrec.id/index.php/bcrec

Bulletin of Chemical Reaction Engineering & Catalysis, 20 (3) 2025, 569-581

Original Research Article

Enhanced Photocatalytic Performance of Ag-Modified ZnO for the Degradation of Tartrazine Dye

Cam Vi Dao Thi[1], Tuan Anh Nguyen[1], Quang Minh Pham[1,2], Anh-Tuan Vu[1,*]

[1]School of Chemistry and Life Sciences, Hanoi University of Science and Technology, Hanoi, Vietnam.
[2]Physico-Chemical Department, National Institute for Control of Vaccine and Biologicals, Vietnam.

Received: 14th July 2025; Revised: 27th August 2025; Accepted: 28th August 2025
Available online: 3rd September 2025; Published regularly: October 2025

Abstract

In this study, ZnO materials were synthesized using the hydrothermal method, and then modified with Ag using glucose, a biologically derived and environmentally friendly reducing agent, to produce Ag/ZnO materials with varying Ag contents. The obtained material samples were characterized using X-ray diffraction (XRD), scanning electron microscopy (SEM), and photoluminescence spectroscopy (PL) to determine the crystal structure, surface morphology, and optical properties, respectively. The results showed that the Ag/ZnO sample containing 5 % Ag (Ag/ZnO-5 %) was able to completely decompose Tartrazine (TA) dye after 80 min of irradiation with an 85 W UV lamp, with a first-order reaction rate constant k = 0.03789 min^{-1} and degradation capacity of 20 mg/g. In comparison, pure ZnO achieved an efficiency of less than 60 %. Factors affecting the photodegradation efficiency, such as initial TA concentration, catalyst dosage, and pH of the solution, were investigated to optimize the reaction conditions. In addition, the Ag/ZnO material exhibited high degradation efficiency toward various organic pollutants, such as Janus Green B (JGB), Congo red (C-Red), Methylene blue (MB), and Caffeine, indicating its potential for broad applications in wastewater treatment. Notably, the investigation of different irradiation light sources (UV, visible light, and sunlight) revealed that sunlight could promote complete degradation of TA in only 20 min of exposure. The photocatalytic reaction mechanism was also proposed to clarify the role of Ag as well as ZnO in enhancing the performance of the Ag/ZnO material system.

Keywords: Tartrazine; ZnO; Ag; Photocatalysis; SPR

How to Cite: Thi, C.V.D., Nguyen, T.A., Pham, Q. M., Vu, A.-T. (2025). Enhanced Photocatalytic Performance of Ag-Modified ZnO for the Degradation of Tartrazine Dye. *Bulletin of Chemical Reaction Engineering & Catalysis*, 20 (3), 569-581. (doi: 10.9767/bcrec.20443)

Permalink/DOI: https://doi.org/10.9767/bcrec.20443

1. Introduction

Environmental pollution caused by the presence of synthetic dyes is currently a significant problem and is increasing rapidly. Most of these dyes have complex molecular structures, are difficult to biodegrade, leading to the ability to persist in the environment for a long time. Among them, azo dyes, typically TA, account for about 65 % of the total amount of dyes used in industries due to their advantages of low cost, high solubility, and color fastness in water [1]. However, besides the advantages in terms of application, TA also has many potential toxic risks, not only negatively affecting human health but also seriously contributing to water pollution. Therefore, many methods have been studied and applied to treat TA in wastewater such as coagulation, adsorption, advanced oxidation, and biological treatment. However, each method has certain disadvantages such as creating a large amount of secondary sludge, the ability to reuse materials or being ineffective for difficult-to-decompose compounds such as TA. Notably, photocatalysis is considered one of the effective dye treatment methods, thanks to its ability to decompose organic compounds that are difficult to

* Corresponding Author.
Email: tuan.vuanh@hust.edu.vn (A.T. Vu)

decompose under suitable light conditions, through the use of a variety of semiconductors as catalysts. However, this method still has certain limitations due to the properties of the catalyst, such as high band gap energy, small specific surface area, and low reusability, which affect the treatment efficiency and practical application [2].

Zinc oxide (ZnO) is a semiconductor material widely used in photocatalysis due to its high stability, low cost, and ability to decompose organic compounds under UV light. Recently, a study on ZnO-NPs synthesized from eucalyptus extract showed 76.1 % TA degradation efficiency under visible radiation, and after 6 recycling cycles, the efficiency decreased by only 6 % [3]. The 10TiO_2/ZnO composite also showed TA degradation ability up to 87.93 % by UV irradiation using sol-gel powder annealed at 500 °C [4]. Moreover, ZnO is often combined with many other materials such as g-C_3N_4 [5,6], Boron [7], to improve the efficiency of treating difficult-to-decompose organic substances. For example, the MB degradation efficiency of ZnO/g-C_3N_4 composite reached 93.2 %, which was higher than that of ZnO and g-C_3N_4 [8]. The ZnO/TiO_2 composite with 3 % B doping achieved tetracycline hydrochloride (TCH) degradation efficiency up to 96.3 % with a rate constant of 0.067 min^{-1} and maintained at 69.7 % after 3 reuse cycles [9]. In particular, the addition of precious metals by taking advantage of the surface plasmon resonance phenomenon or the formation of a Schottky barrier has significantly enhanced the catalytic efficiency. In particular, Ag/ZnO-10 synthesized by a simple precipitation method can completely decompose BPA after 120 min of irradiation under visible light thanks to the improvement in light absorption and photogenerated charge separation efficiency [10]. Or there has been a study showing that the photocatalytic activity in the visible light region of Ag/ZnO nanoparticles is significantly improved by the process of Ag deposition onto the ZnO surface using the laser induction method, achieving a maximum MB decomposition efficiency of up to 92 % [11]. These results show that the combination of Ag and ZnO is a potential photocatalytic material in the treatment of difficult-to-decompose organic pollutants.

In this study, Ag/ZnO materials were synthesized by the hydrothermal method combined with biological reduction by glucose. The photocatalytic activity was investigated through the ability to decompose TA and some difficult-to-decompose organic substances under different illumination conditions. In addition, factors affecting the reaction efficiency such as pH, pollutant concentration, catalyst mass, and light source were also considered to aim at practical applications in wastewater treatment.

2. Materials and Method

2.1 Materials

Zinc nitrate hexahydrate ($(Zn(NO_3)_2.6H_2O$, 99.5 %), silver nitrate ($AgNO_3$, 99.9 %), urea ($(NH_2)_2CO$, 99.5 %), polyvinylpyrrolidone (PVP, $(C_6H_9NO)_n$, 99 %) and D-(+)-glucose ($C_6H_{12}O_6$, 99%), Tartrazine ($C_{16}H_9N_4Na_3O_9S_2$, 99 %), Caffeine ($C_8H_{10}N_4O_2$, 99 %), Janus Green B ($C_{30}H_{31}N_6Cl$, 99 %), Congo red (C-Red, $C_{32}H_{22}N_6Na_2O_6S_2$, 99 %), Methylene Blue ($C_{16}H_{18}ClN_3S$, 99 %), ethylene diamine tetra acetic acid EDTA ($C_{10}H_{16}N_2O_8$, 99 %), ascorbic acid (AA, $C_6H_8O_6$, 99 %), isopropyl alcohol (IPA, C_3H_8O, 99%), were purchased from Merck. None of the reagents required further purification before use.

2.2 Synthesis of ZnO and Ag/ZnO samples

The synthesis of ZnO by a simple hydrothermal method is shown in Figure 1(a). First, 30 mL of 0.5 M $Zn(NO_3)_2.6H_2O$ solution was added to a 250 mL glass beaker containing 70 mL of distilled water. Then, 1.8018 g of $(NH_2)_2CO$ was added to the solution. The mixture was stirred for 30 min at room temperature to ensure homogeneity. Next, the solution was transferred to a hydrothermal reactor at 90 °C for 24 h. After the reaction, the product was filtered using a vacuum pump. The precipitate was then washed several times with distilled water to remove impurities and subsequently dried at 90 °C for 24 hours. Finally, the sample was calcined at 400 °C for 2 h at a heating rate of 2 °C/min to obtain crystalline ZnO material.

The synthesis procedure of Ag/ZnO materials was as follows in Figure 1(b). First, 0.324 g ZnO was added to a beaker containing 40 mL of distilled water, then 1 g of glucose and 0.2 g of PVP were added to the mixture. The mixture was heated at 60 °C for 10 min to completely dissolve. Then, an $AgNO_3$ solution with $AgNO_3$/ZnO molar ratios varying from 2 to 10 % was added to the mixture. The reduction of Ag^+ and deposition of Ag particles onto the ZnO surface were carried out at 60 °C for 1 h under continuous stirring. The obtained product was filtered, washed several times with distilled water, and dried at 60 °C overnight. The Ag/ZnO samples with silver contents of 2, 5, 7, and 10 wt% were named as Ag/ZnO-2%, Ag/ZnO-5%, Ag/ZnO-7%, and Ag/ZnO-10%, respectively.

2.3 Characteristics

The crystal structure of the material was determined by X-ray diffraction (XRD) using a Bruker D8 Advance instrument with Cu-Kα radiation, operating at 40 kV and 40 mA. The surface morphology of the material was observed by scanning electron microscopy (SEM). The

photoluminescence (PL) spectrum was measured at an excitation wavelength of 325 nm to investigate the emission properties and defect states in the ZnO substrate.

2.4 Photocatalytic Experiment

The photocatalytic degradation of TA was carried out as follows: first, 0.05 g of catalyst was added to 100 mL of 10 mg/L TA solution, and the mixture was ultrasonicated to disperse the material evenly. Next, the reaction was carried out for 80 min under irradiation of a 15W UV lamp. A UV-Vis spectrophotometer (Agilent 23 8453) was used to determine the residual TA concentration every 10 min at a wavelength of 430 nm. The following formulas were used to determine the rate constant (k), degradation capacity (Q), and degradation efficiency (DE) of the dyes:

$$\ln\left(\frac{C_0}{C_t}\right) = k \times t \quad (1)$$

$$DE(\%) = \frac{C_0 - C_t}{C_O} \times \quad (2)$$

$$Q\left(\frac{\text{mg}}{\text{g}}\right) = \frac{C_0 - C_t}{m} \times V \quad (3)$$

where k is the pseudo-first-order rate constant; C_0 and C_t are the concentrations of dye at initial (t = 0) and time t (min), respectively; V is the volume of dye solution (L); and m is the mass of the adsorbent (g).

3. Results and Discussion

3.1 Effect of Ag Contents

Figure 2 illustrates the effects of light irradiation, catalysts, and varying Ag contents on the TA degradation efficiency. In Figure 2(a), the experiment was conducted without light to investigate the adsorption/desorption equilibrium time for the Ag/ZnO-5 % sample. The results show that shows that the TA adsorption capacity

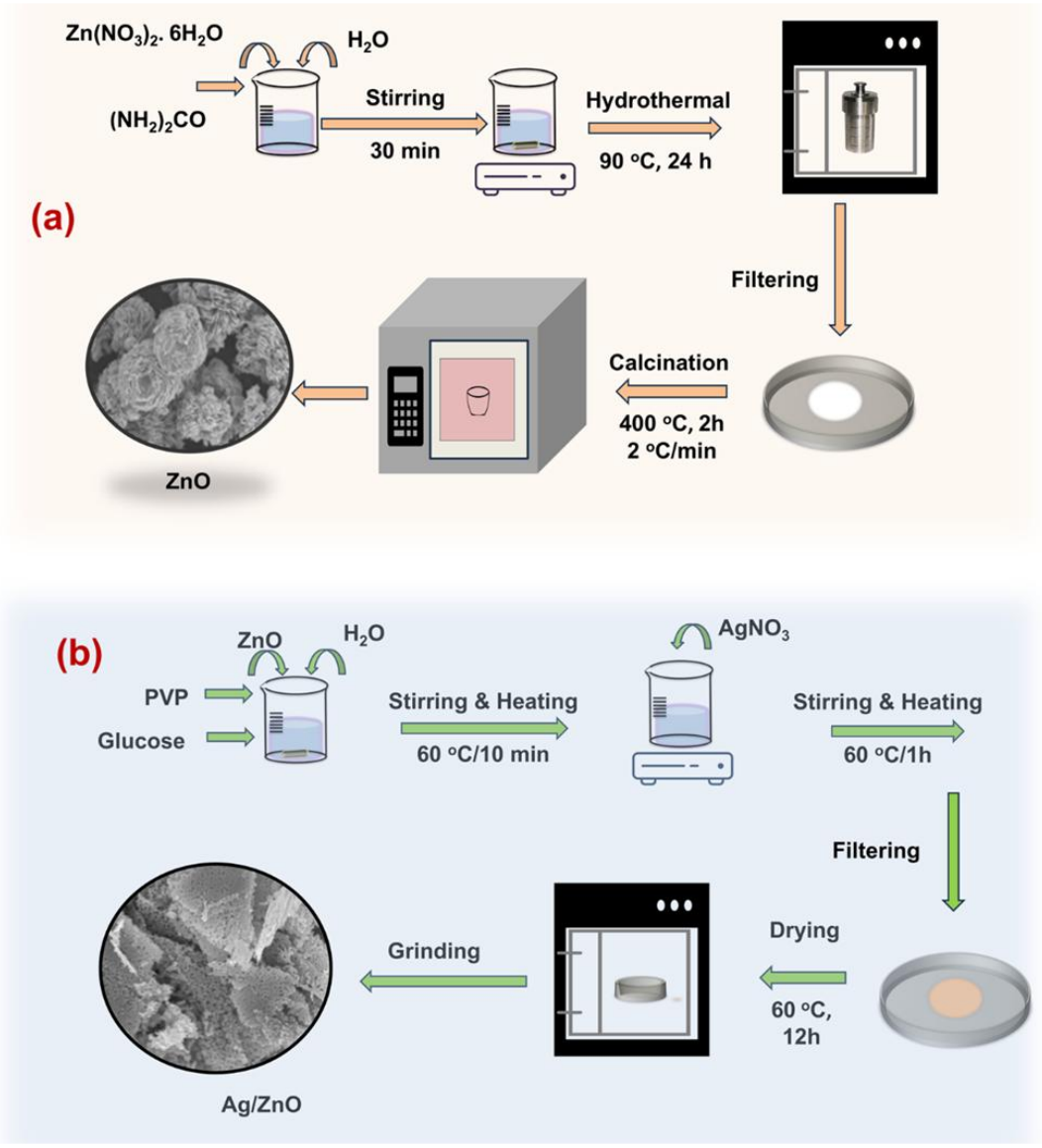

Figure 1. Synthesis of (a) ZnO and (b) Ag/ZnO.

reached about 10 % in the first 10 min, and then the adsorption almost does not change. Therefore, the adsorption equilibrium time was set to 10 min. The above investigation indicated the important role of light irradiation and proved that TA degradation is photocatalytic. The Ag/ZnO-5 and 7 % materials showed almost complete decomposition after 80 min, while the pure ZnO gave a significantly lower efficiency of about 60 %. However, when the Ag content increased to 10 %, the catalytic efficiency decreased compared to the 5 vs 7 % samples, indicating that too high Ag content may hinder the photocatalytic process, possibly by covering the catalyst surface or impairing the separation of e^- h^+ pairs. The kinetics of TA degradation followed a pseudo-first-order model. The results in Figure 2(b) show that the Ag/ZnO-5 % material had the largest rate constant (k = 0.03789 min^{-1}), followed by 0.03390, 0.02580, 0.01278 min^{-1} of Ag/ZnO-7, 10, and 2 %, respectively. Meanwhile, pure ZnO had very small rate constants (k ≈ 0.01134 min^{-1}), reflecting significantly lower photocatalytic performance. In addition, the study of TA adsorption capacity in Figure 2(c) also shows that as the Ag content increases from 2 to 5 %, the adsorption capacity increases sharply from 12 mg/g to reach its highest value of approximately 20 mg/g at 5-7 % Ag. However, when the Ag content continues to increase to 10 %, the adsorption capacity tends to decrease slightly. It can be seen that increasing the Ag content to 7 % only slightly improves or maintains the efficiency, while exceeding the threshold of 10 % reduces both the absorption capacity and degradation efficiency compared to the 5 % doped sample. Therefore, Ag/ZnO-5 % was selected as the optimal photocatalytic material. Figure 2(d) shows the UV-Vis absorption spectrum of TA using the Ag/ZnO-5 % sample over the illumination time. The characteristic absorption peak of TA at around 430 nm gradually decreased and almost disappeared after 80 min, indicating a sharp decrease in the dye concentration over time. This result confirms the strong degradation efficiency of the Ag/ZnO-5 % sample and is consistent with the data on efficiency, kinetics, and absorption capacity presented above.

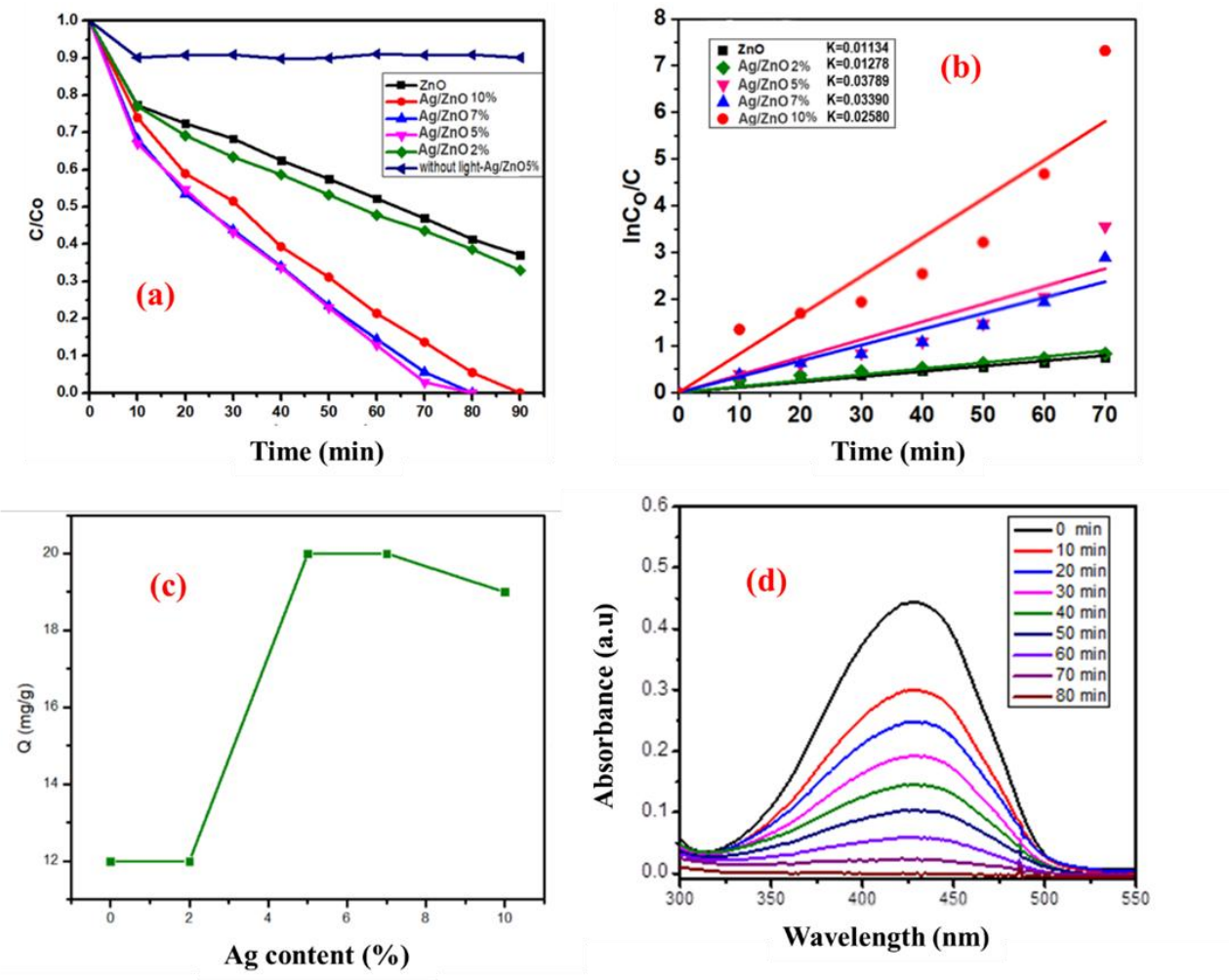

Figure 2. (a) TA decomposition efficiency, (b) the kinetic curves, (c) absorption capacity at different Ag contents, and (d) UV-VIS spectrum of TA decomposition of Ag/ZnO-5 %. Reaction conditions: catalyst dosage of 0.05 g, TA concentration of 10 mg/L.

3.2 Characterizations of the Catalyst

XRD patterns of ZnO and Ag/ZnO-5 % are shown in Figure 3. Both samples show 2θ diffraction peaks of 31.74°, 34.34°, 36.16°, 47.56°, 56.54°, 62.82°, 66.48°, 67.96°, 69.0° corresponding to the (100), (002), (101), (102), (110), (103), (200), (112) and (201) planes of ZnO (JCPDS No. 36-1451) with a hexagonal crystal structure (a = b = 3.250 Å, and c = 5.207 Å) [12]. This contributes to affirm that Ag doping does not affect the crystal lattice structure of ZnO. For the Ag/ZnO-5 % sample, two additional peaks at 2θ = 38.2° and 44.4° appeared, which are characteristic of the (111) and (200) plane diffraction of Ag in the cubic structure (JCPDS No. 04-0783) [13]. In addition, the intensity of the diffraction peaks of the Ag/ZnO-5 % sample was higher than that of the pure ZnO sample, which suggested that Ag doping could help improve the crystallinity or crystal orientation of the ZnO material.

Figure 4 shows the distinct difference in morphology of ZnO and Ag/ZnO-5 %. Pure ZnO in Figure 4(a-b) shows a petal-like structure, consisting of thin layers stacked on top of each other, creating a highly porous and organized structure, contributing to an increase in the specific surface area. Meanwhile, the Ag/ZnO-5 % sample in Figure 4(c-d) has a surface structure that tends to become rougher and less uniform, indicating the influence of Ag doping on the structure formation mechanism, as well as the ability to change the surface properties of the material. In addition, the EDX spectrum of the Ag/ZnO-5 % sample in Figure 5 shows that the composite composition includes 22.04 % O, 73.71 % Zn, and 4.25 % Ag. The EDS mapping results demonstrate the uniform distribution of elements, especially Ag, throughout the ZnO matrix. This confirms the success of the Ag/ZnO synthesis, with well-dispersed Ag, contributing to the improvement of the photocatalytic efficiency of the material.

Figure 6(a-b) shows that both the ZnO and Ag/ZnO-5 % samples exhibit type IV adsorption/desorption isotherms with H3 hysteresis loop, which is typical of mesoporous materials. In addition, Figure (c) shows the pore distributions determined by the Barrett-Joyner-Halenda (BJH) method from the desorption branch of the isotherm. Both samples showed a mixture of pore sizes, but it could be seen that most of the pores possessed a width in the range of 5-60 nm. The Ag/ZnO-5 % sample has a BET surface area of 24.2 m^2/g, which is significantly higher than that of the ZnO sample at 16.0 m^2/g. In addition, the pore volume and average pore size of the Ag/ZnO-5 % sample increased accordingly, to 0.2101 cm^3/g and 32.4 nm, respectively, compared to the ZnO sample with 26.9 nm and 0.155 cm^3/g, as shown in Table 1. These results indicate that the grafting of Ag onto the ZnO matrix in conjunction with the presence of PVP during the synthesis process contributed to a significant improvement in the surface area as

Table 1. Textural properties of ZnO and Ag/ZnO-5 % samples.

Samples	S_{BET} (m^2/g)	Pore volume (cm^3/g)	Average pore size (nm)
ZnO	16.0	-	26.9
Ag/ZnO-5 %	24.2	0.2101	32.4

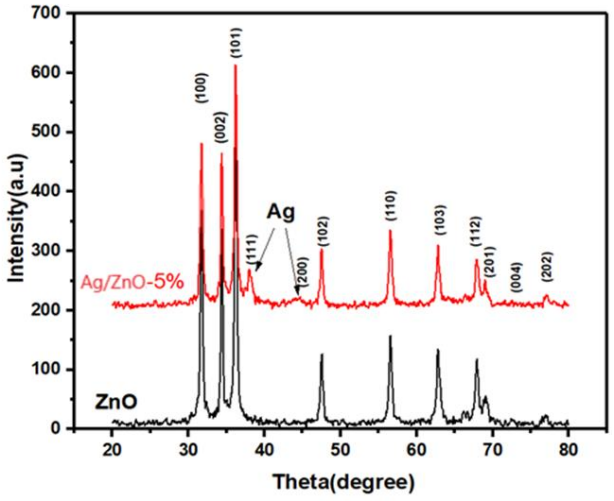

Figure 3. XRD of ZnO and Ag/ZnO-5 % samples.

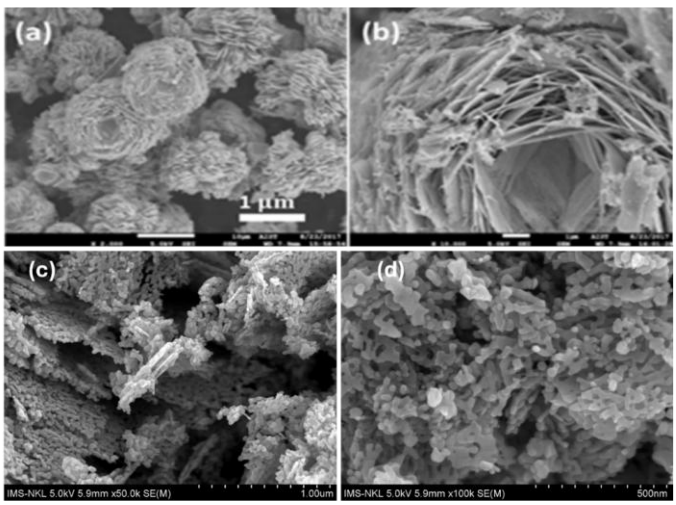

Figure 4. SEM images of (a-b) ZnO, and (c-d) Ag/ZnO-5 % samples.

well as the mesoporous properties of the material. This improvement not only helps to increase the adsorption capacity, but also improves the contact between the catalyst and the dye, thereby enhancing the photocatalytic reaction efficiency.

The UV-Vis diffuse reflectance spectra of ZnO and Ag/ZnO-5 % are shown in Figure 7(a). Pure ZnO exhibits a characteristic absorption edge in the ultraviolet region (around 380 nm), which is consistent with the characteristics of a wide bandgap semiconductor [14,15]. After doping with AgNPs, the absorption edge of Ag/ZnO-5 % significantly broadened to the visible light region, indicating an improvement in light absorption efficiency. This is attributed to the SPR effect of Ag nanoparticles, which enhances the absorption in the visible light region and supports more efficient e^-/h^+ pair separation. In addition, AgNPs act as mediators of electron transfer, reducing recombination and promoting electronic interactions with ZnO. This interaction can lead to the formation of interband gaps or improve the electronic coupling between the conduction and valence bands. Figure 7(b) shows the Tauc plot used to determine the band gap energy (E_g) of the material. The Eg value calculated by the Tauc method shows that the ZnO material has an E_g of about 3.17 eV, while the E_g of Ag/ZnO-5 % is reduced to 3.11 eV. It is assumed that the uniform distribution and low content of AgNPs are responsible for the low gap energy of the composite material. This slight decrease reflects the change in the energy band structure after doping with AgNPs and contributes to the increase in light absorption and enhanced photocatalytic activity under sunlight.

PL analysis was performed to evaluate the charge carrier separation efficiency of the catalysts as shown in Figure 8. Pure ZnO exhibits a strong emission peak in the visible region of 680-700 nm. This peak is attributed to the deep emission level, mainly associated with point defects in the ZnO crystal lattice. Specifically, oxygen vacancies and interstitial Zn atoms are

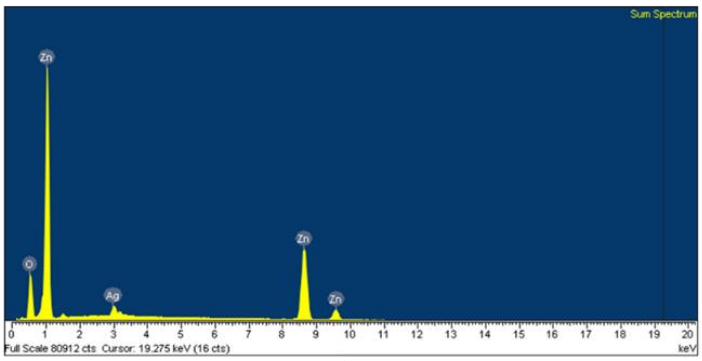

Element	Weight%	Atomic%
O K	22.04	54.13
Zn K	73.71	44.32
Ag L	4.25	1.55
Totals	100.00	

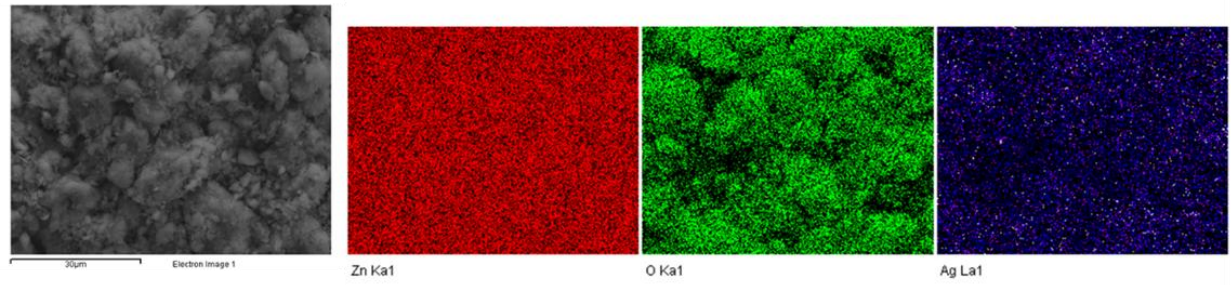

Figure 5. EDX-mapping results of Ag/ZnO-5 % sample.

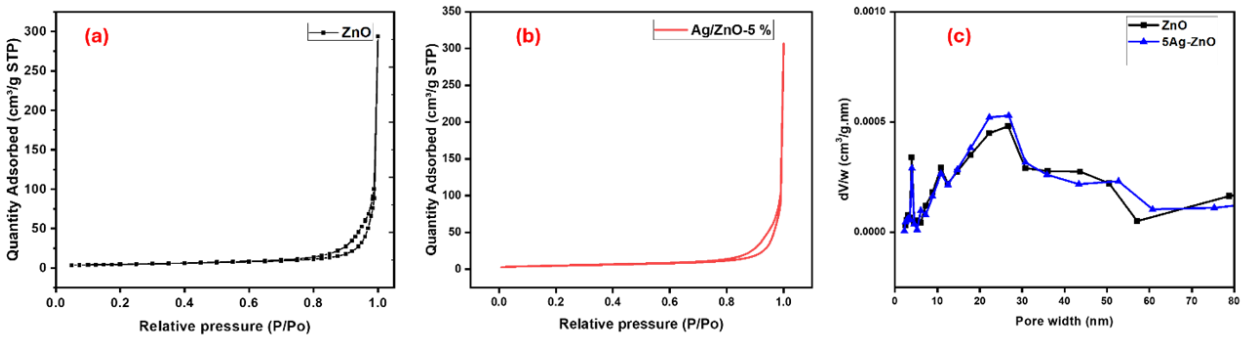

Figure 6. (a-b) N_2 adsorption/desorption isotherms and (c) pore size distribution of ZnO and Ag/ZnO-5 % samples.

considered to be the main causes of the creation of energy levels in the band gap, which leads to emission in the long-wavelength region [16]. Meanwhile, the Ag/ZnO-5 % sample showed a significant decrease in luminescence intensity. This decrease indicates the formation of intermediate energy levels due to Ag doping, which changes the kinetics of the e^-/h^+ recombination process. Electrons in the excited state tend to move to these intermediate levels instead of recombining directly with holes in the valence band, as in the pure ZnO sample. Therefore, Ag doping has contributed to reducing the recombination efficiency, increasing the lifetime of charge carriers, and thereby improving the photocatalytic performance of the material.

3.3 Effect of Initial TA Concentration and Catalyst Dosage

Figure 9(a-b) shows the effect of TA concentration on photodegradation efficiency. When the TA concentration increased from 5 mg/L to 30 mg/L, the degradation efficiency and

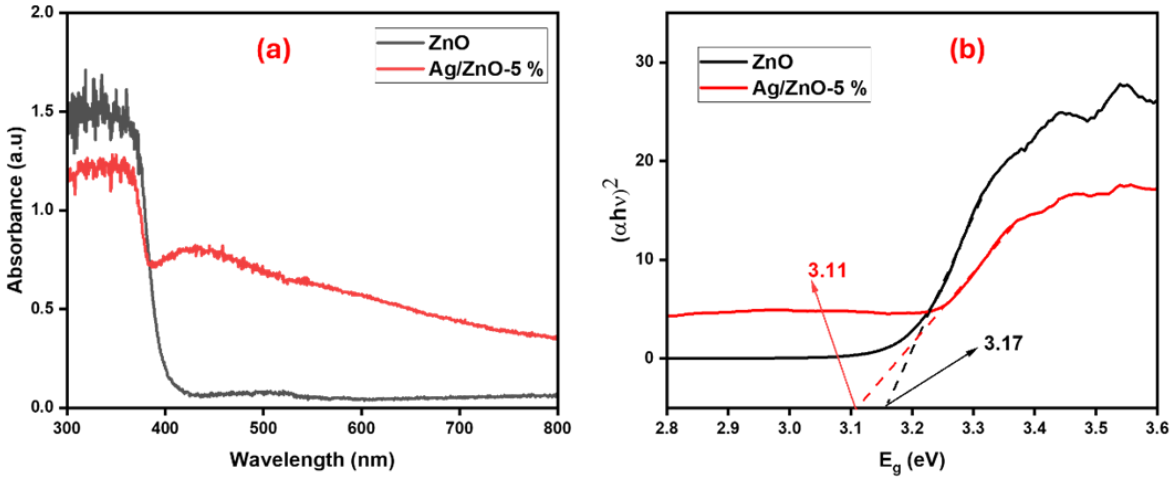

Figure 7. (a) DR/UV-vis and (b) Tauc's plots of ZnO and Ag/ZnO-5 %.

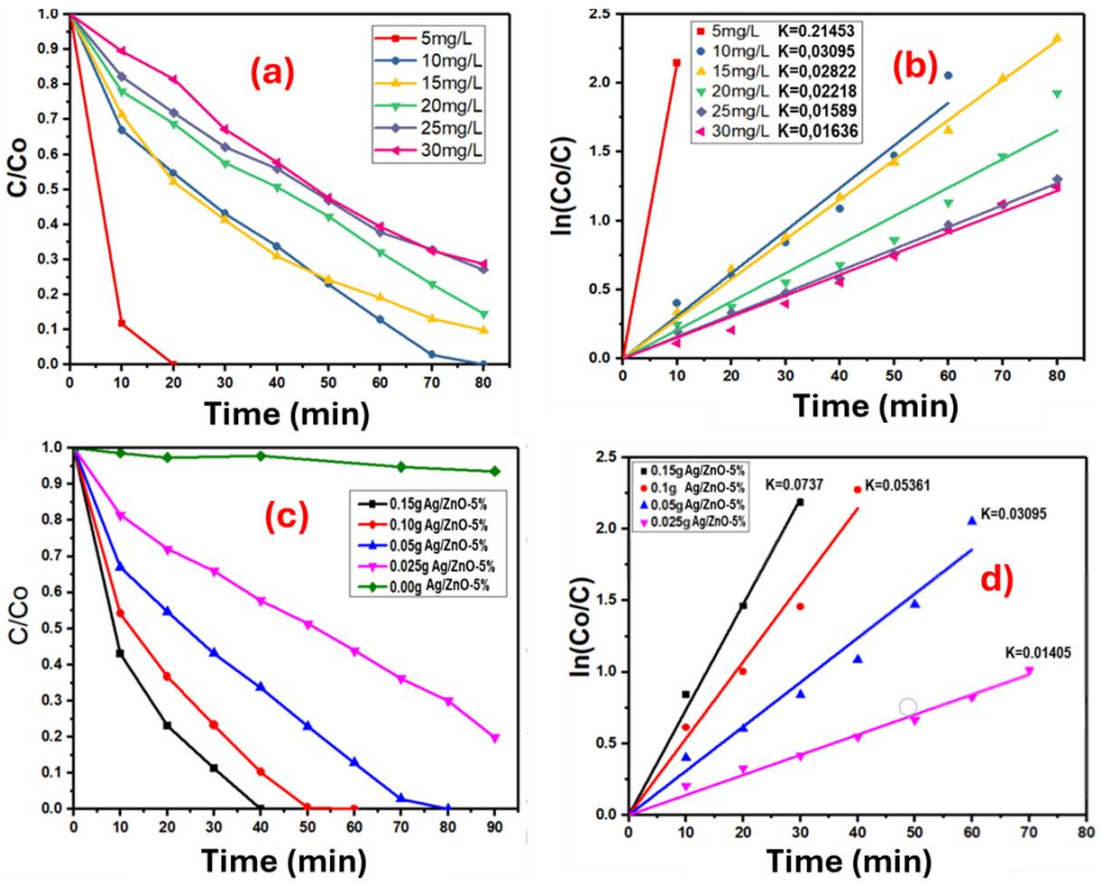

Figure 9. (a-b) Effect of initial dye concentration and fitting plots at different initial concentrations of TA, and (c-d) effect of catalyst dosage and fitting plots at different catalyst dosages.

reaction rate decreased significantly. This phenomenon can be explained by the fact that at lower concentrations, the catalyst surface has more available active sites, leading to the excessive formation of hydroxyl radicals, while at high concentrations, TA molecules tend to saturate the catalyst surface, limiting the ability to absorb light and generate ·OH radicals necessary for the degradation process. Besides, Figure 9(c-d) illustrates the effect of Ag/ZnO-5 % mass fraction on the degradation efficiency. In the absence of a catalyst, there is almost no degradation of TA, but when the catalyst amount is increased to 0.15 g, the degradation efficiency increases significantly. This result demonstrates that increasing the catalyst mass provides more active sites and a larger surface area, which enhances the adsorption and generation of active oxygen radicals. However, at an optimal value, increasing the catalyst concentration too much can cause photo-occlusion or particle agglomeration, reducing the photo-dispersion efficiency.

3.4 Effect of pH Solution

The influence of the reaction environment plays a very important role in the photocatalytic process, which is demonstrated through photodegradation experiments at different pH conditions. Figure 10 shows that the highest degradation efficiency is achieved in an alkaline environment (pH = 11), while in an acidic environment (pH = 4), the efficiency decreases significantly. At the same time, the Tadegradation capacity also tends to increase gradually with pH, from about 17 to nearly 20 mg/g. The improvement in efficiency in an alkaline environment can be explained as follows: at high pH, the catalyst surface carries a stronger negative charge, thereby easily interacting with positively charged or neutral TA molecules, increasing the adsorption capacity and enhancing the catalytic activity. In addition, the alkaline environment also promotes the formation of ·OH through photochemical reactions, contributing to enhanced pollutant degradation ability. On the contrary, in an acidic environment, part of ZnO may be dissolved, degrading the catalyst structure and leading to lower decomposition efficiency according to the following equation: $ZnO + 2H^+ \rightarrow Zn^{2+} + H_2O$.

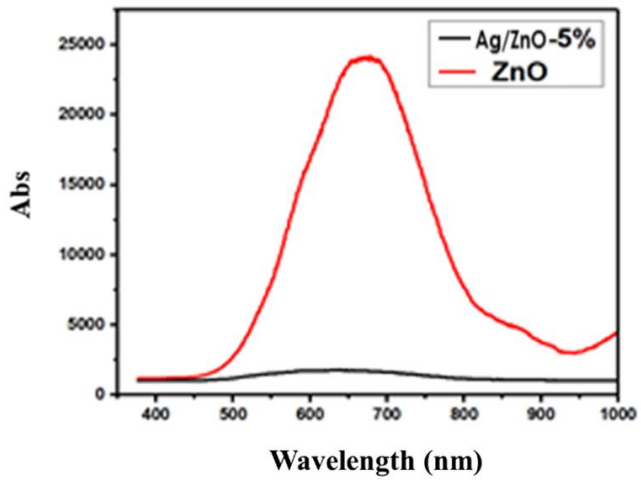

Figure 8. PL spectrum of ZnO and Ag/ZnO-5 % samples.

3.5 Degradation of Different Organic Pollutants

The photodegradation process is not limited to TA but also extended to other organic substances. The results in Figure 11 show that the ability to decompose organic substances is quite good, in which C-Red is decomposed the fastest, reaching almost a complete level after only 10 min of illumination. Next are JGB and TA, with a strong decomposition rate and almost reaching the elimination threshold after 60-70 min. For Caffeine, the decomposition process is slower but still shows a steady decreasing trend over time. In contrast, MB is the substance with the lowest decomposition rate, with more than 50 % of the concentration remaining after 80 min, indicating a weak interaction between MB and the catalyst surface. C-Red and TA have high adsorption capacities (20 mg/g), while MB and Caffeine have lower values (14-16.5 mg/g). This shows the wide application potential of Ag/ZnO-5 % material in

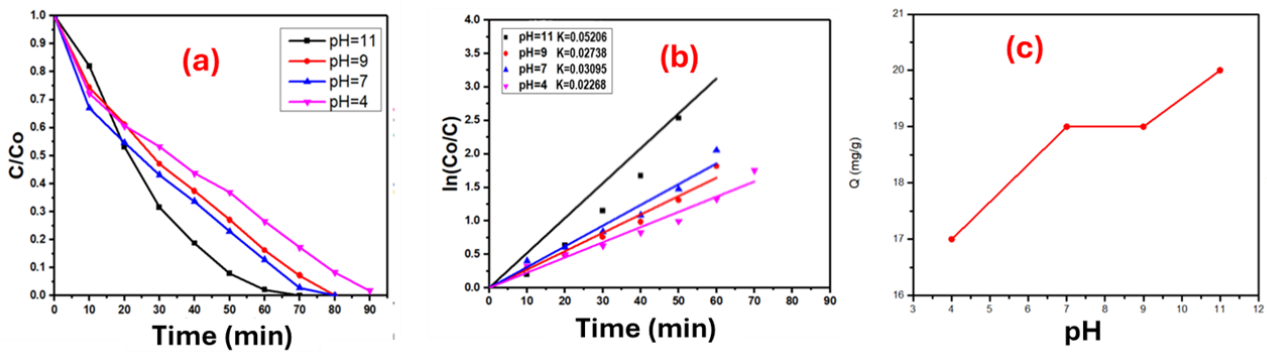

Figure 10. (a) Effect of pH solution, (b) fitting plots, and (c) the degradation capacity at different pH values.

wastewater treatment containing organic dyes, especially effective with substances such as C-Red, TA, and JGB.

3.6 Effect of Different Light Irradiation

The degradation efficiency of organic dye TA by Ag/ZnO-5 % material is affected by the illumination conditions as shown in Figure 12. Among the investigated light sources, sunlight gives superior degradation efficiency, with TA almost eliminated after only 10 min. UV light also gives high efficiency, reaching almost complete elimination after about 80 min. Meanwhile, 200 W visible light is the least effective condition, with only about 40 % TA decomposed after 80 min. The superiority of sunlight can be explained by two main factors. First, the doping of Ag into the ZnO structure improves the ability to absorb light in the visible region through the surface plasmon resonance (SPR), while also acting as effective electron traps, thereby reducing the recombination of e^-/h^+ pairs and improving the efficiency of free radical generation for the degradation process. Second, the intensity of sunlight is significantly higher than that of artificial sources such as UV or LED lights, contributing to the acceleration of the photocatalytic reaction. This confirms the potential application of the material under outdoor natural light conditions for the sustainable treatment of wastewater containing organic matter.

Table 2 shows the photocatalytic performance of the synthesized catalysts in this study compared to some previously reported composite materials for TA degradation. The results show that the Ag/ZnO-5 % sample exhibits comparable degradation performance, even surpassing many published material systems, demonstrating the high potential application of this material in the treatment of difficult-to-degrade organic pollutants. In addition, the reusability of Ag/ZnO-5 % nanocomposite was investigated through 4

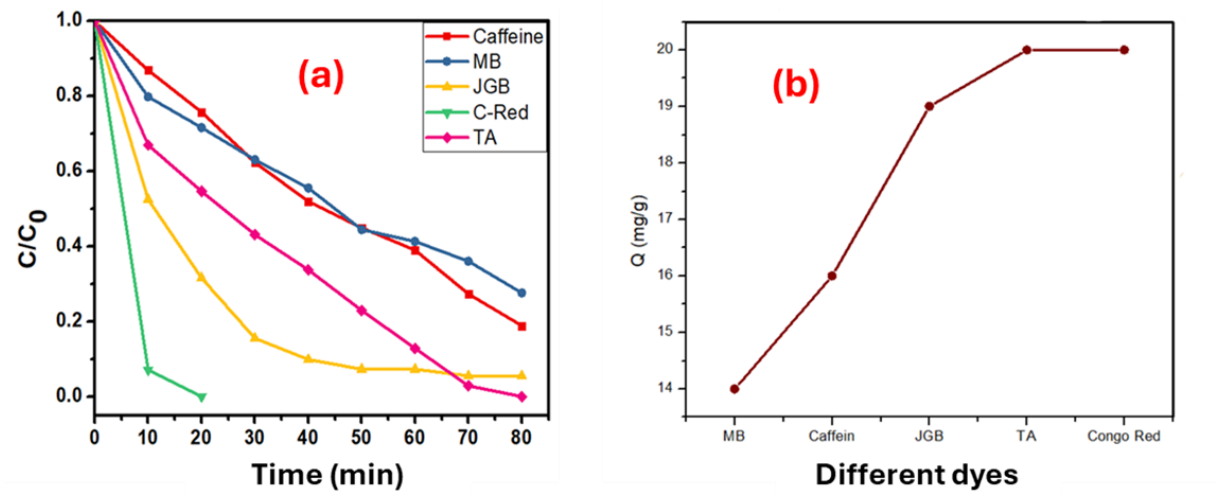

Figure 11. (a) Degradation efficiency and (b) degradation capacity of the different organic pollutants.

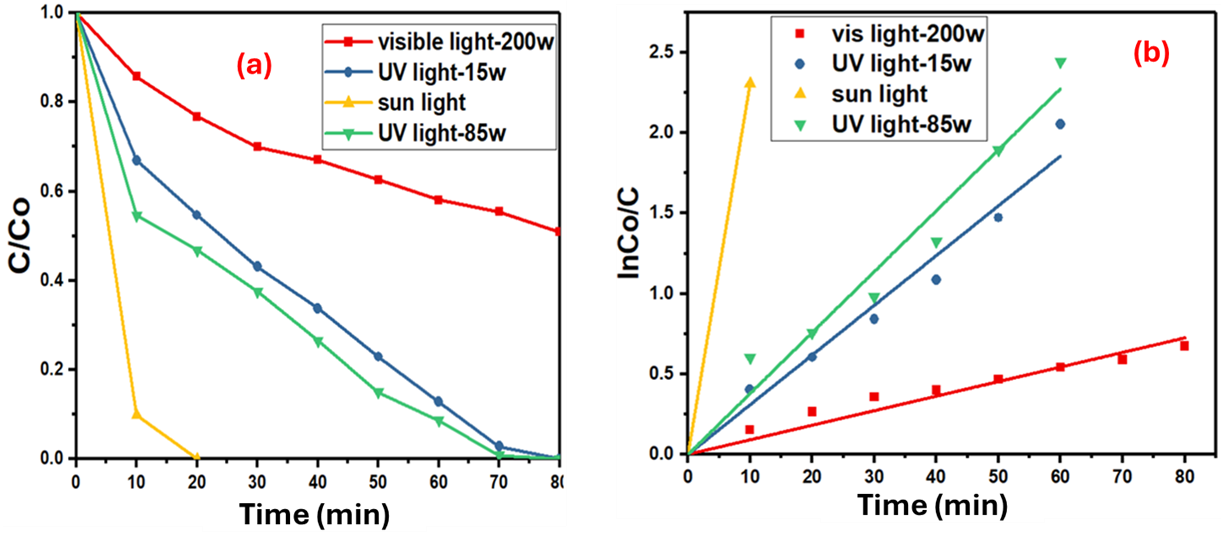

Figure 12. (a) Effect of light irradiation on TA degradation, and (b) fitting plots.

cycles to evaluate the photocatalytic efficiency and application potential of the material. The results presented in Figure 13 show that the photocatalytic efficiency of TA degradation decreased from 99.8 to 90.5, 82.6, and 78.5 % after each cycle. This can be explained by the loss of active sites and the increase of intermediates on the catalyst surface, which decreased the performance of the catalyst.

3.7 Photocatalytic Degradation Mechanism

The role of free radicals in the photocatalytic process was also investigated by adding radical scavengers, such as $AgNO_3$, EDTA, AA, and IPA, to capture the radicals e^-, h^+, $\cdot O_2^-$, and $\cdot OH$, respectively [17-21]. The results are shown in Figure 14. When EDTA was added, the TA degradation efficiency decreased drastically to about 20 %. This indicates that EDTA is the main active species, that plays a key role in the TA oxidation process. The addition of IPA and AA decreased the efficiency to about 30-33 %, indicating that both the hydroxyl radicals $\cdot OH$ and $\cdot O_2^-$ also play an important agents in the degradation process. In contrast, the presence of $AgNO_3$ only decreased the efficiency to about 55 %, suggesting that e^- mainly played an indirect role in maintaining the charge balance and supporting e^-/h^+ separation, rather than directly participating in the TA oxidation reaction. The studies showed that the above free radicals were the main agents in the photocatalytic degradation of TA on Ag/ZnO-5 % materials. Based on the above results, a proposal for a photocatalytic degradation mechanism is presented.

Experimental results show that Ag/ZnO materials exhibit significantly superior photocatalytic performance compared to pure ZnO in the degradation of organic dye TA. The mechanism of this enhanced efficiency mainly comes from the ability to inhibit the recombination between e^- and h^+ pairs, as well as the SPR effect characteristic of Ag nanoparticles, which helps to extend the light absorption region to the visible region, especially near UV light, as shown in Figure 15. When ZnO absorbs photons with suitable energy, electrons are excited from the valence band to the conduction band, creating e^-/h^+ pairs. These charged particles can react with oxygen and water molecules on the catalyst surface to generate strong oxidizing agents, such

Table 2. Comparison of the degradation of TA by various materials.

Catalyst	Reaction conditions	DE (%)	Refs.
5 mol% Ni-CeO_2	[Cat.] = 1 g/L, [TA]= 10^{-4} M, UV irradiation, 360 min	65.4	[23]
30$LaFeO_3$/ZnO	[Cat.] = 3 g/L, [TA]=10 mg/L, UV light, 180 min	84	[24]
Au/ZnO/Fe_3O_4	[Cat.] = 0.25 g/L, [TA]=5 mg/L, Hg lamp 250 W, 60 min, 12 mM H_2O_2	81.5	[25]
Ag-T_2	[Cat.] = 0.3 g/L, [TA]=10 mg/L, Xenon light source, 180 min	87	[26]
(Ce,Ag)/ZnO	[Cat.] = 1 g/L, [TA]=10 mg/L, pH = 6, sunlight iradiation, 90 min	98.91	[27]
Ag/ZnO-5 %	[Cat.] = 0.5 g/L, [TA]=10 mg/L, pH = 7, 15 W UV light, 70 min	100	This study

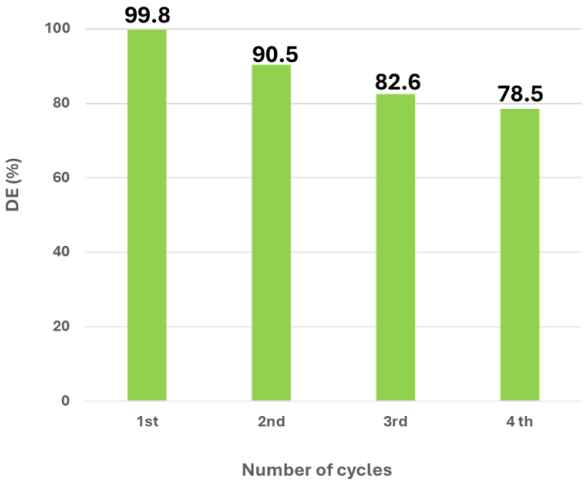

Figure 13. The recycling of Ag/ZnO-5 %.

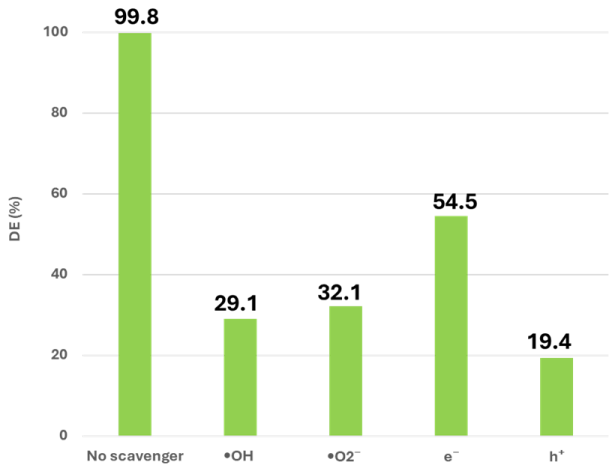

Figure 14. Effect of different scavengers on the Ag/ZnO-5 % catalyzed photocatalytic degradation of TA.

as ·OH and $\cdot O_2^-$, which play a major role in breaking down complex organic bonds in TA molecules. However, in pure ZnO, electrons in the conduction band often quickly recombine with holes, which degrades the catalytic performance. When Ag is doped, a Schottky barrier is formed at the Ag/ZnO interface due to the Fermi energy difference, allowing electrons from ZnO to move to Ag, where they are retained, preventing recombination. As a result, electrons on Ag continue to react to form $\cdot O_2^-$ radicals, while holes in ZnO promote the formation of ·OH radicals, improving the TA decomposition efficiency. At the same time, the presence of Ag also helps absorb light more effectively, especially under sunlight, a source of radiation with high intensity and a wide spectrum, thereby optimizing the catalytic efficiency of the material. The photocatalytic reaction is described as follows:

$$ZnO + h\nu \rightarrow ZnO\ (e^-) + h^+ \quad (4)$$
$$ZnO\ (e^-) + Ag \rightarrow ZnO + Ag\ (e^-) \quad (5)$$
$$Ag\ (e^-) + O_2 \rightarrow \cdot O_2^- + Ag \quad (6)$$
$$2\cdot O_2^- + 2H_2O \rightarrow H_2O_2 + 2OH^- + 2O_2 \quad (7)$$
$$e_{CB}^- + H_2O_2 \rightarrow \cdot OH + OH^- \quad (8)$$
$$ZnO\ (h^+) + H_2O \rightarrow ZnO + H^+ + \cdot OH \quad (9)$$
$$h^+ + OH^- \rightarrow \cdot OH \quad (10)$$
$$\cdot O_2^- / \cdot OH + TA \rightarrow \text{Intermediate products} \rightarrow CO_2 + H_2O \quad (11)$$

Although the TA degradation efficiency reached nearly 100 % after photocatalytic treatment, this does not guarantee that the intermediate products generated are completely harmless. Therefore, the identification of intermediate compounds and their toxicity assessment are necessary to better understand the reaction mechanism and environmental safety. Dos Santos *et al.* studied the fragmentation of TA photodegradation products and proposed a scheme for TA photodegradation under UV light based on the structures determined by LC-ESI-MS/MS. Table 3 lists some by-products of this TA degradation process [22].

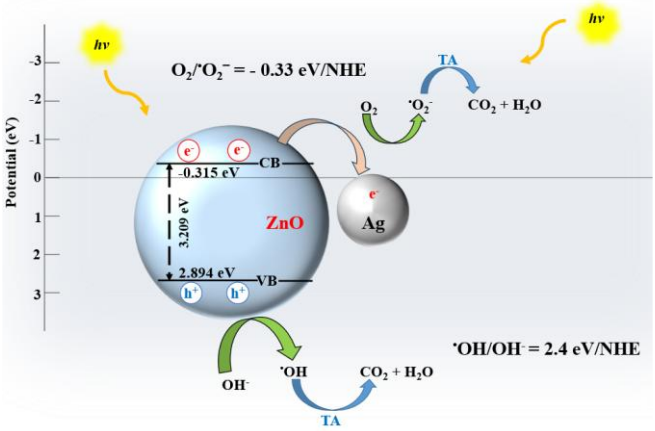

Figure 15. Photocatalytic mechanism of TA degradation of Ag/ZnO.

4. Conclusion

Ag/ZnO materials were successfully synthesized by the reduction method using glucose, an environmentally friendly biological reducing agent, showing potential for application in the development of sustainable photocatalytic systems. In particular, Ag/ZnO-5 % material achieved TA degradation efficiency of up to 100 % after 80 min of UV light illumination and after only 20 min under sunlight. The addition of Ag to the ZnO structure plays a key role in improving the photocatalytic efficiency. Ag particles not only act as an effective electron trap, helping to prevent the recombination of electron-hole pairs, but also improve the ability to absorb light thanks to the SPR effect. As a result, Ag/ZnO materials can exploit light more effectively, thereby improving the ability to decompose difficult-to-degrade organic pollutants, showing high potential for application in wastewater treatment. In future studies, non-precious metals such as Cu or Fe could be considered as potential alternatives to Ag to reduce cost while maintaining photocatalytic performance. Additionally, optimizing the synthesis parameters or developing hybrid photocatalysts based on Ag/ZnO may further improve their activity and adaptability to different environmental conditions.

Table 3. Some intermediate products of TA decomposition.

Product	Proposed Structure
I	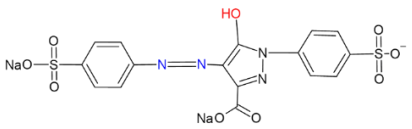
II	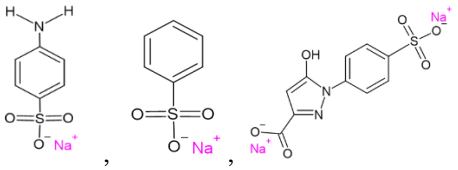
III	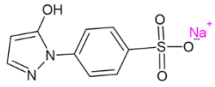
IV	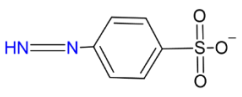
V	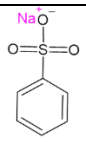

Acknowledgments

The work was performed at the Analysis and Testing Laboratory, School of Chemistry and Life Sciences, Hanoi University of Science and Technology. Cam Vi Dao Thi was funded by the Master, PhD Scholarship Programme of Vingroup Innovation Foundation (VINIF), code VINIF.2024.ThS.21.

CRedit Author Statement

Author Contributions: Cam Vi Dao Thi: data curation, formal analysis, investigation, methodology, visualization, writing - original draft, Tuan Anh Nguyen: investigation, methodology, Quang Minh Pham: investigation, methodology, Anh-Tuan Vu: supervision, validation, writing - review & editing. All authors have read and agreed to the published version of the manuscript.

References

[1] Micheletti, D.H., da Silva Andrade, J.G., Porto, C.E., Alves, B.H.M., de Carvalho, F.R., Sakai, O.A., Batistela, V.R. (2023). A review of adsorbents for removal of yellow tartrazine dye from water and wastewater. *Bioresource Technology Reports*, 24, 101598. DOI: 10.1016/j.biteb.2023.101598

[2] Gupta, V.K., Jain, R., Nayak, A., Agarwal, S., Shrivastava, M. (2011). Removal of the hazardous dye—Tartrazine by photodegradation on titanium dioxide surface. *Materials Science and Engineering: C*, 31(5), 1062-1067. DOI: 10.1016/j.msec.2011.03.006

[3] Wouters, R.D., Muraro, P.C.L., Druzian, D.M., Viana, A.R., de Oliveira Pinto, E., da Silva, J.K. L., *da Silva, J.K.L., Vizzotto, B.S., Ruiz, Y.P.M., Galembeck, A., Pavoski, G., Espinosa, D.C.R.,* da Silva, W. L. (2023). Zinc oxide nanoparticles: Biosynthesis, characterization, biological activity and photocatalytic degradation for tartrazine yellow dye. *Journal of Molecular Liquids*, 371, 121090. DOI: 10.1016/j.molliq.2022.121090

[4] Kaneva, N., Bachvarova-Nedelcheva, A. (2024). The Effect of Heat Treatment on the Sol–Gel Preparation of TiO2/ZnO Catalysts and Their Testing in the Photodegradation of Tartrazine. *Applied Sciences*, 14 (21). DOI: 10.3390/app14219872

[5] Dao Thi, C.V., Nguyen, T.A., Nguyen Thi, T.A., Vu, A.T. (2025). Synthesis of g-C_3N_4-based nanocomposites with low Au loading for efficient methylene blue degradation. *Nanotechnology*. 36 (25), 255703. DOI: 10.1088/1361-6528/ade0c5

[6] Nguyen, T.T.A., Dao, T.C.V., Vu, A.-T. (2024). Controlling the physical properties of Ag/ZnO/g-C3N4 nanocomposite by the calcination procedure for enhancing the photocatalytic efficiency. *Ceramics International*, 50(9), 14292-14306. DOI: 10.1016/j.ceramint.2024.01.336

[7] Nguyen, T.H., Mai, T.T., Tran, T.P., Thi, C.L.T., Thi, C.V.D., Thi, M.L.V., Nguyen, T.M., Luong, N.S., Le, V.D., Nguyen, M.V., Nguyen, T.H., Vu, A.-T. (2024). Studying the nanocomposite B/ZnO for photocatalysis: facile control the morphology via sol-gel method and antibiotic degradation investigations. *Journal of Sol-Gel Science and Technology*, 110(2), 319-332. DOI: 10.1007/s10971-024-06359-z

[8] Vu, A. (2020). Synthesis of ZnO, g-C3N4 and ZnO/g-C3N4 composite and their photocatalytic activity under vilsible light irradiation. *Vietnam Journal of Catalysis and Adsorption*, 9(2), 87-93. DOI: 10.51316/jca.2020.034

[9] Nguyen, T.H., Vu, A.-T. (2024). Investigation of enhanced degradation of the antibiotic under visible in novel B/ZnO/TiO2 nanocomposite and its electrical energy consumption. *Nanotechnology*, 35(1), 015709. DOI: 10.1088/1361-6528/acffce

[10] Pham, T.A.T., Tran, V.A., Le, V.D., Nguyen, M.V., Truong, D.D., Do, X.T., Vu, A.-T. (2020). Facile preparation of ZnO nanoparticles and Ag/ZnO nanocomposite and their photocatalytic activities under visible light. International *Journal of Photoenergy*, 2020(1), 8897667. DOI: 10.1155/2020/8897667

[11] Whang, T.-J., Hsieh, M.-T., Chen, H.-H. (2012). Visible-light photocatalytic degradation of methylene blue with laser-induced Ag/ZnO nanoparticles. *Applied Surface Science*, 258(7), 2796-2801. DOI: 10.1016/j.apsusc.2011.10.134

[12] Vu, A.-T., Nguyen Thi Tu, A., Dao Thi Cam, V. (2025). A Novel Ag/ZnO/g-C3N4 (A/ZCN) Nanocomposite for photocatalytic treatment of organic dyes in aqueous solution. *Environmental Engineering Science*, 42(5), 189-202. DOI: 10.1089/ees.2024.0346

[13] Tuấn, V.A., Minh, P.Q., Anh, N.T.T., Vi, Đ.T.C., Hằng, N.T.B., Hương, N.T. (2024). Tổng Hợp Vật Liệu Ag/ZnO/g-C3N4 Bằng Phương Pháp Nung Đơn Giản Để Loại Bỏ Kháng Sinh Tetracycline Hydrochloride Trong Môi Trường Nước. *Journal of Control Vaccines and Biologicals*, 4(1). DOI: 10.56086/jcvb.v4i1.142

[14] Natsume, Y., Sakata, H., Hirayama, T. (1995). Low-temperature electrical conductivity and optical absorption edge of ZnO films prepared by chemical vapour deposition. *Physica Status Solidi (A)*, 148(2), 485-495. DOI: 10.1002/pssa.2211480217

[15] Wu, C., Shen, L., Zhang, Y.C., Huang, Q. (2012). Synthesis of AgBr/ZnO nanocomposite with visible light-driven photocatalytic activity. *Materials Letters*, 66(1), 83-85. DOI: 10.1016/j.matlet.2011.08.030

[16] Alenezi, M.R., Henley, S.J., Emerson, N.G., Silva, S.R.P. (2014). From 1D and 2D ZnO nanostructures to 3D hierarchical structures with enhanced gas sensing properties. *Nanoscale*, 6(1), 235-247. DOI: 10.1039/C3NR04519F

[17] Dao Thi, C.V., Nguyen, T.A., Nguyen Thi, T.A., Vu, A.-T. (2025). Synthesis of g-C3N4-based nanocomposites with low Au loading for efficient methylene blue degradation. *Nanotechnology*, 36(25), 255703. DOI: 10.1088/1361-6528/ade0c5

[18] Bodannes, R. S., & Chan, P. C. (1979). Ascorbic acid as a scavenger of singlet oxygen. *FEBS Lett*., 105(2), 195-196. DOI: 10.1016/0014-5793(79)80609-2

[19] Ding, L., Hou, Y., Liu, H., Peng, J., Cao, Z., Zhang, Y., Wang, B., Cao, X., Chang, Y., Wang, T., Liu, G., Wang, T. (2023). Alcohols as scavengers for hydroxyl radicals in photocatalytic systems: reliable or not? *ACS ES&T Water*, 3(11), 3534-3543. DOI: 10.1021/acsestwater.3c00271

[20] Labaran, B., Vohra, M. (2014). Photocatalytic removal of selenite and selenate species: effect of EDTA and other process variables. *Environmental Technology*, 35(9), 1091-1100. DOI: 10.1080/09593330.2013.861857

[21] Samsudin, M.F.R., Siang, L.T., Sufian, S., Bashiri, R., Mohamed, N.M., Ramli, R.M. (2018). Exploring the role of electron-hole scavengers on optimizing the photocatalytic performance of BiVO4. *Materials Today: Proceedings*, 5(10), 21703-21709. DOI: 10.1016/j.matpr.2018.07.022

[22] dos Santos, T.C., Zocolo, G.J., Morales, D.A., Umbuzeiro, G.d.A., Zanoni, M.V.B. (2014). Assessment of the breakdown products of solar/UV induced photolytic degradation of food dye tartrazine. *Food and Chemical Toxicology*, 68, 307-315. DOI: 10.1016/j.fct.2014.03.025

[23] Ali, S.R., Kumar, R., Kadabinakatti, S.K., Arya, M.C. (2018). Enhanced UV and visible light—driven photocatalytic degradation of tartrazine by nickel-doped cerium oxide nanoparticles. *Materials Research Express*, 6(2), 025513. DOI: 10.1088/2053-1591/aaee44

[24] Vaiano, V., Iervolino, G., Sannino, D. (2016). Photocatalytic removal of tartrazine dye from aqueous samples on LaFeO3/ZnO photocatalysts. *Chemical Engineering Transactions*, 52, 847-852. DOI: 10.3303/CET1652142

[25] Quang, L.V., Vu, A.-T. (2023). Preparation of Au/ZnO/Fe3O4 composite for degradation of tartrazine under visible light. *Bulletin of Chemical Reaction Engineering & Catalysis*, 18(1), 71-84. DOI: 10.9767/bcrec.17061

[26] Ratshiedana, R., Fakayode, O.J., Mishra, A.K., Kuvarega, A.T. (2021). Visible-light photocatalytic degradation of tartrazine using hydrothermal synthesized Ag-doped TiO2 nanoparticles. *Journal of Water Process Engineering*, 44, 102372. DOI: 10.1016/j.jwpe.2021.102372

[27] Bouarroudj, T., Aoudjit, L., Djahida, L., Zaidi, B., Ouraghi, M., Zioui, D., Mahidine, S., Shekhar, C., Bachari, K. (2021). Photodegradation of tartrazine dye favored by natural sunlight on pure and (Ce, Ag) co-doped ZnO catalysts. *Water Science and Technology*, 83(9), 2118-2134. DOI: 10.2166/wst.2021.106.